Hindawi Publishing Corporation
Journal of Nanomaterials
Volume 2016, Article ID 4961714, 8 pages
http://dx.doi.org/10.1155/2016/4961714

Hindawi

Research Article

Magnetoelectric Effect in Type-II Quantum Cone Induced by Donor Impurity

L. F. Garcia,[1] I. D. Mikhailov,[1] and J. Sierra-Ortega[2]

[1]*Universidad Industrial de Santander, A. A. 678, Bucaramanga, Colombia*
[2]*Grupo de Investigación en Teoría de la Materia Condensada, Universidad de Magdalena, Santa Marta, Colombia*

Correspondence should be addressed to L. F. Garcia; lfragar@gmail.com

Received 14 July 2016; Accepted 18 August 2016

Academic Editor: Javad Foroughi

We consider a model of donor centered at the base of a type-II nanocone, in which the excessive electron, released from the donor, is located within a narrow tube-shaped shell exterior region around the cone lateral surface. By solving the one-electron Schrödinger equation we analyze the alteration of the spatial probability distribution of the electron, the period of the Aharonov-Bohm oscillations of the energy levels, and the electric and magnetic moments induced by external electric and magnetic fields, applied along the symmetry axis. We show that the diamagnetic confinement provided by the magnetic field forces the electron to climb along the cone's border, inducing the electric polarization of the structure. Similarly, the external electric field, which pushes the electron toward cone's bottom, changes the order of the energy levels with different magnetic momenta varying the magnetic polarization of the structure. Our theoretical analysis reveals a new possibility for the coupling between the polarization and magnetization arising from the quantum-size effect in type-II semiconductor nanocones.

1. Introduction

The magnetoelectric effect is the phenomenon of inducing magnetic (electric) polarization by applying an external electric (magnetic) field that has been revealed previously in ceramics, crystals, and epitaxial crystalline layers, composites of piezoelectric and magnetostrictive particles in laminated layers [1]. The possibility of controlling magnetization and/or polarization by an electric field and/or magnetic field allows an additional degree of freedom in device design [2]. The aim of this paper is to call attention to a possibility of existence of a similar coupling between the polarization and magnetization semiconductor nanocone provided by the quantum confinement in quasi-one-dimensional nanostructures such as wires, cones, or rods.

The quasi-1D structures have a natural architecture for light trapping and therefore at present are considered as a promising choice for optoelectronic devices such as solar cells and photodetectors [3, 4]. A reduced dimensionality that retains a single conducting channel in quasi-1D structures makes them very sensible to the external electric field with respect of any process related to the separation of positive and negative charges. The charge separation in a nanostructure can be additionally reinforced by a type-II heterojunction, constructed from two materials for which both the edges of the valence and conduction bands of one component are lower than those in the other component. Nanowires with type-II heterojunctions core/shell like ZnO/ZnSe have been synthesized for solar cell applications [5], in which the hole states are more confined in the cylindrical core component and the electron states are more confined in the tube-shaped shell component. Radii of the core of ZnO nanowires are typically 60–120 nm and thickness of ZnSe shell is 5–8 nm [5].

Earlier studies have been reported on fabrication of different types of nonvertically aligned GaN/GaP core/shell nanowires [6] and particularly one of them with type-II heterojunction, between cone-shaped GaN core and a thin tube-shaped GaP shell [6]. In this paper we intend to prove that such structure can exhibit the magnetoelectric effect. To this end we consider, as an example, a simple model of an on-axis shallow donor in type-II semiconductor nanocone. The excessive electron released from the donor is mainly located within a thin shell region, encompassing the cone-shaped antidot, a region forbidden for the electron for penetrate

inside. In the presence of a strong external magnetic field, the excessive electron circulates around the nanocone being localized inside a narrow region.

The possible electron's paths within this region with convex topology have an important particularity related to their extraordinary sensibility to external magnetic field. The interaction between the magnetic field and circular electric current induced by this field pushes the electron toward the axis while the confinement, provided by the antidot barrier and the external magnetic field, retains it outside of the nanocone, making possible only circular paths encompassing the antidot. It gives rise to a set of special properties of the energy spectrum typical for the Aharonov-Bohm (AB) effect, which is characterized by oscillations of curves of the energies dependencies on the magnetic field and periodic multiple crossovers between them. Previously, AB effect has been studied for narrow QRs with one and two electrons [3] and with neutral and charged excitons [7–11].

AB effect in a structure with cone-shaped morphology has particular peculiarities, related to an additional degree of freedom acquired by the electron along the symmetry axis within the shell region. In the presence of the external magnetic field parallel to the symmetry axis the probability distributions of the electron, in states with different angular momenta, are defined by the interplay between the centrifugal and diamagnetic forces.

The centrifugal force pushes the maxima of the electron distributions with different angular momenta toward the cone's bottom, while the diamagnetic force drives them to the cone top. As the magnetic field is weak, the predominant centrifugal force retains the electron rotation around the axis close to the bottom. When the magnetic field is increased, the peaks of the electron distributions corresponding to different angular momenta begin to climb successively one by one from the bottom toward the top in the order of ascending angular momenta pushed up by the diamagnetic force. Such redistribution of the electron's probability density under external magnetic field produces an electric polarization of the structure along the symmetry axis.

Similar alteration of the magnetic polarization occurred in the presence of the electric field applied parallel to the cone axis. A sufficiently strong electric field can suppress or reinforce the escalation of rotational trajectories, induced by the magnetic field, reordering the energy levels corresponding to different magnetic momenta and changing the magnetization of the system.

The paper is organized as follows. In the next section we describe a procedure of separation of variables of the one-particle wave equation for an on-axis shallow donor in a type-II semiconductor nanocone, in which the excessive electron released from the donor is mainly located within a thin shell region, encompassing the cone-shaped antidote.

Numerical results for dependencies of the energies, magnetic and electric momenta, and susceptibilities on the external magnetic and electric fields presented in Section 3 reveal a new possibility for the coupling between the polarization and magnetization arising from the quantum-size effect in type-II semiconductor nanocones. Finally some conclusions are presented in Section 4.

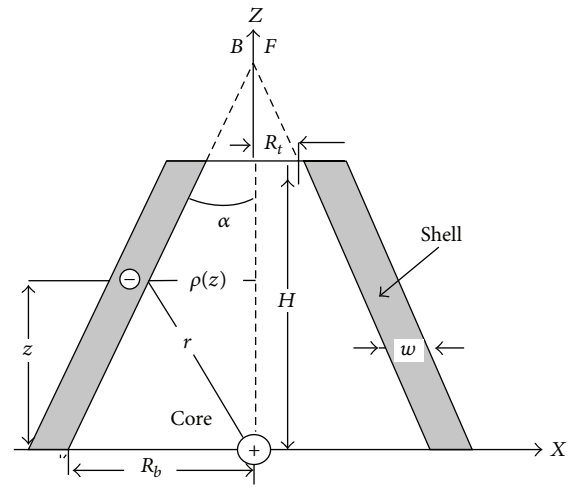

Figure 1: Vertical cross-section of a type-II nanocone with on-axis donor.

2. Theoretical Model

We consider a nanometric architecture, with the vertical cross-section along the symmetry axis schematically represented in Figure 1, where the donor impurity is located at the center of the bottom of a type-II nanocone with geometrical parameters given by the height H, the bottom and the top radii of the conical cores R_b and R_t, respectively, and the shell thickness w. The external homogeneous fields, magnetic field B, and electrical field F are applied parallel to the Z axis. The core region of the structure is regarded below as an infinite-barrier antidot, whose lateral frontier surface is given in cylindrical coordinates by the dependence:

$$\rho(z) = R_b - (R_b - R_t) \cdot \frac{z}{H}. \quad (1)$$

This surface presents a hard wall for the electron released from the on-axis donor, located at the core bottom. The magnetic field B applied parallel to the Z axis presses the electron inside the shell region to the wall. Therefore, one can expect that the electron is mainly located within the quasi-2D region:

$$\{\rho(z) < r < \rho(z) + w;\ 0 < z < H,\ 0 < \varphi < 2\pi\} \quad (2)$$

in which the electron circulates around the core, encompassing the cone's lateral surface.

In our calculations we use the effective Bohr radius $a_0^* = \hbar^2\varepsilon/m^*e^2$, the effective Rydberg, $R_y^* = e^2/2\varepsilon a_0^*$, the parameters $\xi = eFa_0^*/R_y^*$, $\gamma = e\hbar B/2m^*R_y^*$ as units of length and energy, and the dimensionless electric F and magnetic B fields, respectively, with m^* being the electron effective mass and ε the dielectric constant of the shell material parameters. Below, we adopt a simple model, in which the excessive electron, released from the donor, is constrained within the shell's region under the confinement potential, equal to zero inside the shell region and to infinity, otherwise. Besides, we take into account that the effective Bohr magneton inside the shell material is significantly larger

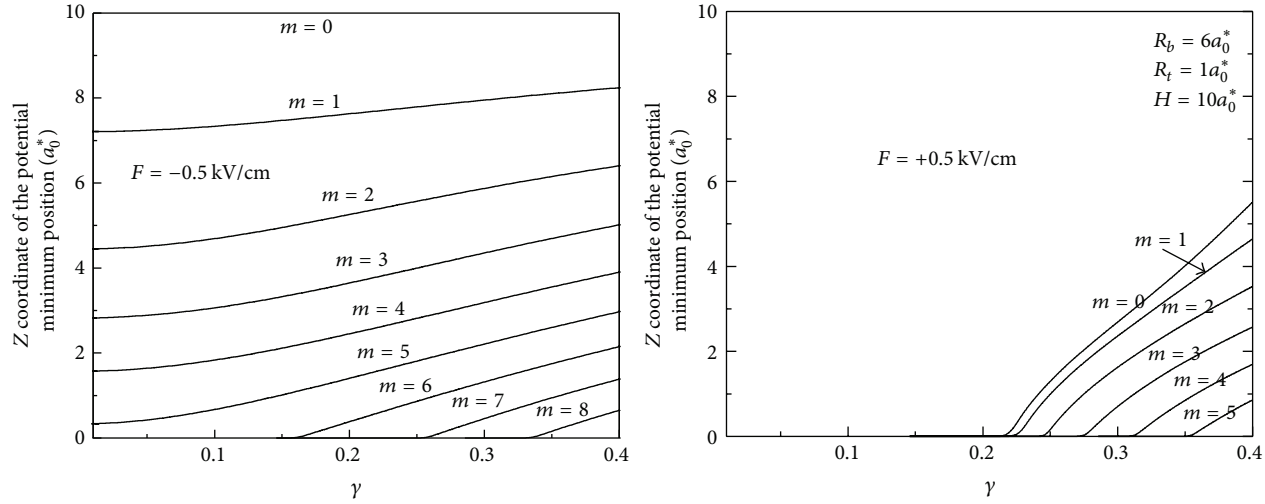

FIGURE 2: Climb of the position of the adiabatic potential minimum along Z axis under increasing magnetic field for three different values of the electric field for lower states of one electron in a conical nanotube with dimensions $R_b = 6a_0^*$, $R_t = 1a_0^*$, and $H = 10a_0^*$.

than the correspondent to spin value and therefore in what follows we consider the spineless Hamiltonian in which the interaction of the magnetic field with the spin is depreciated. Due to the axial symmetry of the structure, the Z-projection m of the angular momentum is a good quantum number and the corresponding donor wave function in cylindrical coordinates can be represented as follows:

$$\Psi_m(r,\varphi,z) = e^{im\varphi}\psi_m(r,z); \quad m = 0, \pm 1, \pm 2, \ldots. \tag{3}$$

By using substitution $r = \tilde{r} + \rho(z)$ and separating the angular variable in 3D one can obtain the following wave equation for donor wave function $\psi_m(r,z)$ in the state with the Z-projection m of the angular momentum:

$$\left[-\frac{1}{\tilde{r}}\frac{d}{d\tilde{r}}\tilde{r}\frac{d}{d\tilde{r}} + V_m\left(\tilde{r}+\rho(z),z\right)\right]\psi_m(\tilde{r},z) + \left[-\frac{\partial^2}{\partial z^2} + \xi\cdot z\right]\psi_m(\tilde{r},z) = E\psi_m(\tilde{r},z),$$
$$V_m(r,z) = \left(\frac{m}{r} - \frac{\gamma r}{2}\right)^2 - \frac{2}{\sqrt{r^2+z^2}}; \quad 0 < z < H;\ 0 < \tilde{r} < w;\ r = \tilde{r} + \rho(z). \tag{4}$$

Below we analyse only a limit case of a very thin shell ($r \lesssim w \to 0$), taking into account that thicknesses of experimentally fabricated type-II nanowires are essentially smaller than their radii [5, 6]. In this limit, one can neglect the displacement of the electron in the radial direction, reducing in this way the 2D eigenvalue problem for $\psi_m(\tilde{r},z)$ to simpler 1D wave equation for $f_m(z) = \lim_{\tilde{r}\to 0}\psi_m(\tilde{r},z)$

$$-\frac{d^2 f_m(z)}{dz^2} + U_m(z) f_m(z) = E\cdot f_m(z); \quad 0 < z < H;\ f_m(0) = f_m(H) = 0, \tag{5}$$

where

$$U_m \approx \xi\cdot z + \left[\frac{m}{\rho(z)} - \frac{\gamma\cdot\rho(z)}{2}\right]^2 - \frac{2}{\sqrt{z^2+\rho^2(z)}}. \tag{6}$$

Eigenenergies of (5) depend on two quantum numbers, axial ($n = 0, 1, 2, \ldots$) and angular ($m = 0, \pm 1, \pm 2, \ldots$). The correspondent eigenfunctions $f_{m,n}(z)$ define the probability density distribution of the electron along the symmetry axis and the dipolar momentum. In our numerical work we solve (6) with potential (7) by using the numerical trigonometric sweep method [12] and we find the lower electron energies $E_{m,n}$ for twenty different magnetic quantum numbers $m = 0, -1, -2, \ldots, -19$ and only one axial quantum number $n = 1$. Below, we present results of calculations for the conical nanotube with geometrical parameters, the base radius $R_b = 6a_0^*$, the height $H = 10a_0^*$, and the top radius $R_t = 1a_0^*$.

3. Results and Discussion

Possible classical paths corresponding to potential (6) are the circumferences of radii $\rho(z)$ at horizontal planes, located at a distance z away from the bottom of the cone. According to (6) the plane position is defined by interplay between four forces: centrifugal force, which pushes the electron toward the cone bottom, the magnetic confinement that drives it to the cone top, and the Coulomb attraction to the donor and the electric field, which can force the electron at both directions. The analysis of the dependencies of the stationary point position $z_{\min}$ corresponding to the minimum of the potential $U_m(z)$ (which defines the position of the classical horizontal circular track) on the external fields allows us to give below a simple interpretation of the spectral, electric, and magnetic properties of the structure.

In Figure 2 we present the displacements of z-positions of potential's minima for some lower states under increasing magnetic field for three different values of the electric field.

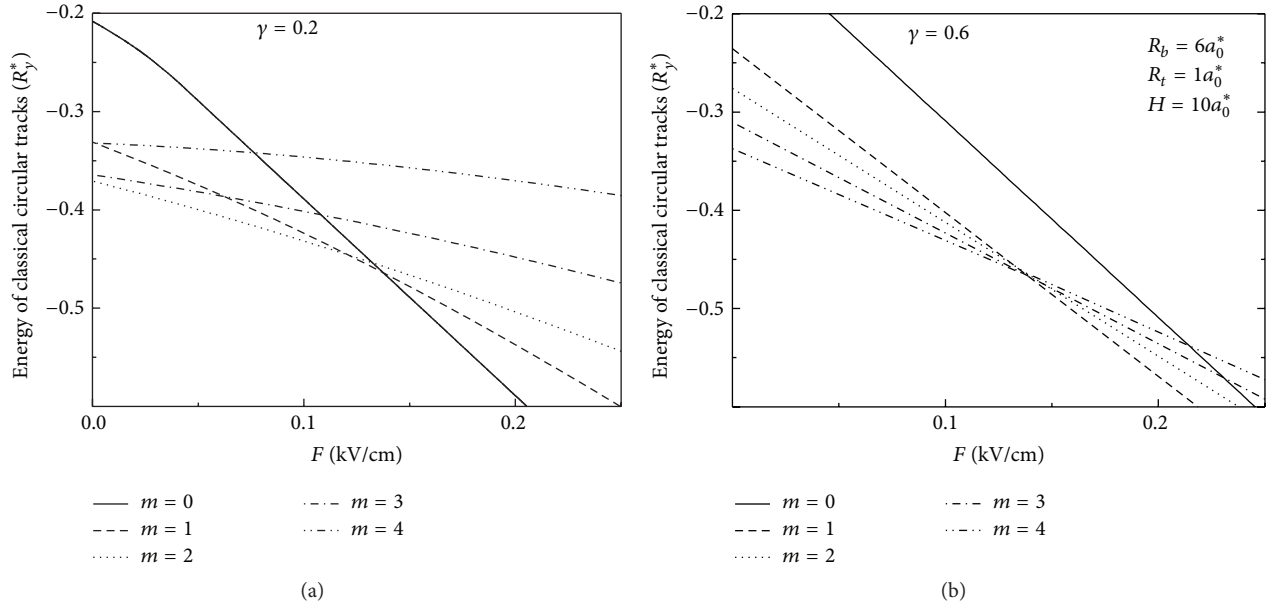

Figure 3: Variation of the minimum energy of the potential (6) for lower rotational states under increasing electric field for three different values of the magnetic field in one-electron conical nanotube with dimensions $R_b = 6a_0^*$, $R_t = 1a_0^*$, and $H = 10a_0^*$.

The z-coordinates of these minima define the corresponding plane of classical circular tracks around of the symmetry axis and, simultaneously, the electron circular tracks around of the symmetry axis and, simultaneously, the classical dipole momentum of the structure, induced by the magnetic field. It is seen from Figure 2 that these tracks are aligned in a sequence of horizontal circular tracks, climbing one by one under increasing magnetic field in ascending order of the angular momentum, from the bottom of the cone toward its top. The number of tracks that participate in this climb between the bottom and the top of the nanotube at the same time depends on the magnetic field value; the larger is the magnetic field the greater is the number of such tracks.

Also, one can see that the external electric field affects essentially the climb of the circular tracks, generated by the external magnetic field, assisting or hindering this process according to the electric field direction. The curves of dependencies of the classical electric polarization of the structure on the external magnetic field, presented in Figure 2, reveal a background for a possible magnetoelectricity in cone-like structures and, besides, they explain how an external electric field could strengthen or weaken this effect.

One would expect a reciprocal relation between the electric and magnetic properties of the structure, according to which the external electric field could also change the initial magnetic polarization. In order to examine such possibility we present in Figure 3, the dependencies of the minimum positions of potential (6) on the electric field in states with different magnetic momenta and for three different values of the external magnetic field. It is seen that the increase of the external electric field provides multiple crossovers of the energies dependencies and the reordering of the energy levels with different angular momenta. The angular momentum of the classical circular track with the lowest energy induced by the external magnetic field in the zero-electric field case increases from $m = 2$ up to $m = 4$ while the magnetic field grows from $\gamma = 0.2$ up to $\gamma = 0.4$.

The crossovers of the curves in Figure 3 are accompanied by the inversion of the energy levels and provide a successive decrease of the magnetic momentum of the ground state and the magnetization of the structure.

In what follows we present the results of calculation of the lower energies as functions of the electric and magnetic fields, obtained by solving the eigenvalue problem (5) by using the trigonometric sweep method [1]. The electric and magnetic momenta p and μ and the susceptibilities χ and χ_m at zero temperature were defined according to the Hellmann-Feynman theorem as

$$\begin{aligned} p &= ea_0^* \cdot \frac{\partial E_1}{\partial \xi}; \\ \chi &= ea_0^* \cdot \frac{\partial^2 E_1}{\partial \xi^2}; \\ p_m &= -\mu_B \cdot \frac{\partial E_1}{\partial \gamma}; \\ \chi_m &= -\mu_B \cdot \frac{\partial^2 E_1}{\partial \gamma^2}. \end{aligned} \tag{7}$$

We calculate by means of the numerical derivation of the ground state energy E_1, μ_B being the effective Bohr magneton and a_0^* the effective Bohr radius.

In Figure 4 we present the lower energies, found by solving eigenvalue problem (5) and parameters of the electric and magnetic polarizations, calculated via relations (7) as functions of the external magnetic field for three different values of the electric field in a nanocone with following

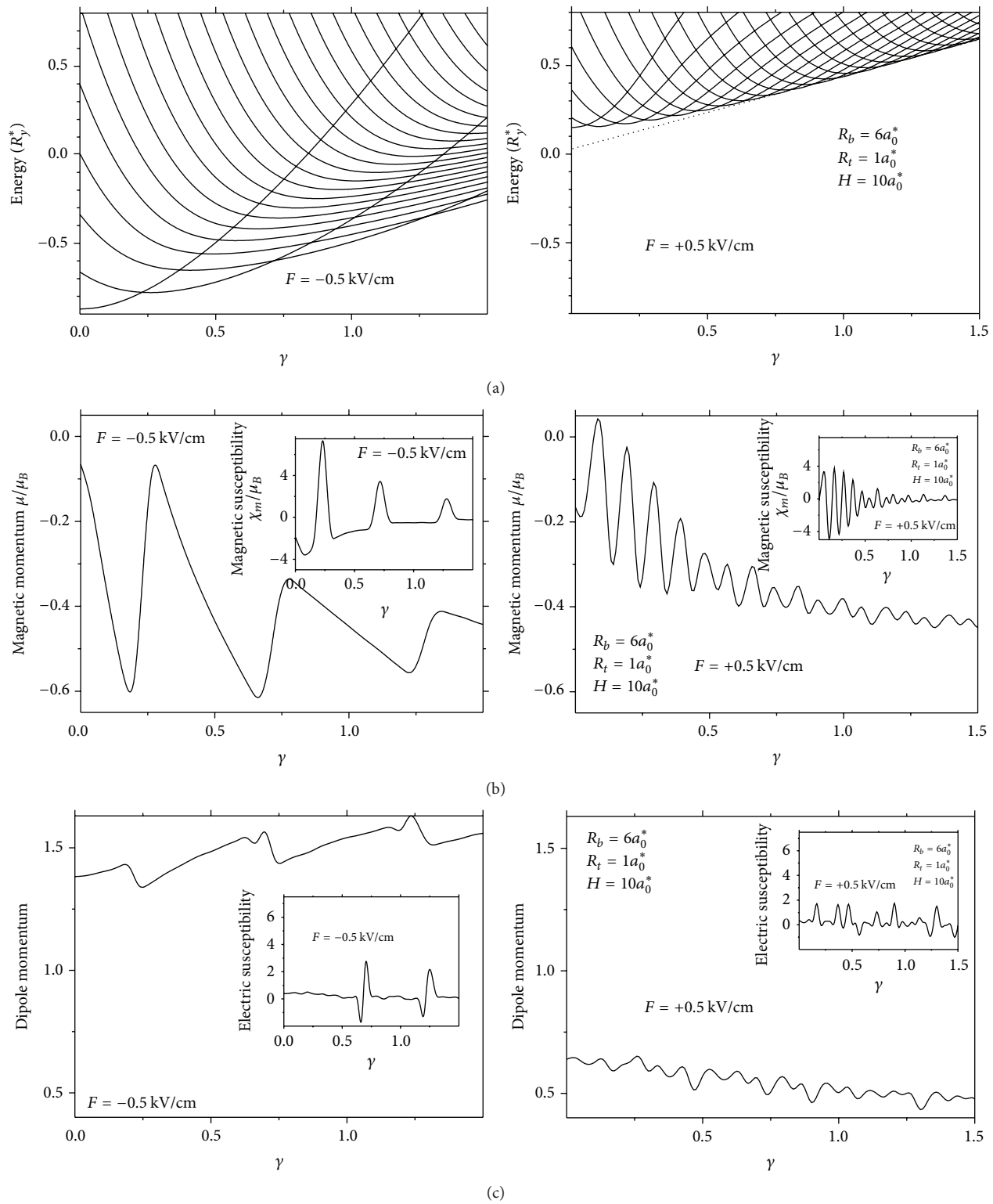

Figure 4: The lower energies and parameters of the electric and magnetic polarizations of an on-axis donor as functions of the external magnetic field in a type-II nanocone with dimensions $R_b = 6a_0^*$, $R_t = 1a_0^*$, $H = 10a_0^*$, and $w = 0.2a_0^*$ for three different values of the electric field.

dimensions, the base radius $R_b = 6a_0^*$, the height $H = 10a_0^*$, and the top radius $R_t = 1a_0^*$.

The oscillatory dependencies of the ground state energies on the magnetic field in curves, presented in the superior row of Figure 4, are different from those in a narrow ring due to the presence of a linear growing trend of the bands' bottoms. The slope of the envelope line over the band bottom for the positive electric field is lesser than for negative one, as it is seen from Figure 4 and it tends to zero in the presence of a very strong electric field.

We attribute such changes of the energy dependency on the magnetic field with a capability of the electric field to obstruct or to stimulate a lifting of the electron circular tracks generated by an increasing magnetic confinement. A very strong positive electric field presses the electron's circular tracks close to the cone's bottom, resulting in transformation of the configuration system to one similar to the 1D quantum ring with radius equal to R_b. Comparing the curves in Figure 4 one can observe that the periods of the oscillation $\Delta\gamma$ for positive and negative electric fields are essentially different. If in the case of the positive electric field $\Delta\gamma$ in Figure 4 is approximately equal to 0.08, that is, slightly exceeding the value $\Delta\gamma = 2/R_b^2$ to the period of AB oscillations in 1D QR of the radius $R_b = 6a_0^*$, while the period $\Delta\gamma$ for the negative electric field in Figure 4 has the value 0.5 that corresponds to the period of AB oscillations in 1D QR of the radius $R = 2a_0^*$, thus, these results demonstrate that the external electric field constrains spatially the probability distribution in the state with lowest energy close to the cone's top if the electric field is negative and about the bottom in the case of the positive field.

The remarkable alteration that induces external electric field over the ground state energy dependence on the magnetic field, which is observed in the curves of the upper row in Figure 4, can provide also a significant change of the polarizability of the structure.

In the following inferior rows we present the curves of the magnetic and electric dipole momenta and susceptibilities as functions of the magnetic field calculated by using relations (7) for negative, positive, and zero-electric field cases. It is seen that all these curves have a form of damped oscillations about an ascent trend line if the electric field is negative and otherwise about a descent trend line. We attribute this conversion of slopes of trend lines of curves in Figure 4 to a relocation of circular tracks of the electron around the symmetry axis, owing to the change of the direction of the electric field. Negative slope of the polarization parameters is associated with a climb of the circular tracks under an increasing magnetic field, which is significant for a positive electric field, when the electron is constrained about the cone's bottom, and vice versa, in the case of negative electric field when the electron is constrained about the cone top.

One can see also that the periods of oscillation related to reordering of the energy levels under increasing magnetic field for the ground state energy in the first row and for all parameters of the magnetic and electric polarizations in inferior rows coincide exactly.

In Figure 5 we present the lower energies, found by solving eigenvalue problem (5), and parameters of the electric and magnetic polarizations, calculated via relations (7) as functions of the external electric field for three different values of the magnetic field ($\gamma = 0, 1, 2$). It is seen that for $\gamma = 0$ there is no crossovers of energy levels and the ground state energy at the first column is increased smoothly with a small change of the slope only for electric fields between -0.2 kV/cm and $+0.2$ kV/cm. Therefore, parameters of polarization have a relatively noticeable alteration only within this interval. One could attribute such dependencies of the polarization parameters to a successive descent of classical circular tracks with different magnetic moments, which have been initially lifted by the negative electric field, toward the cone bottom.

The corresponding dependencies are strongly different for $\gamma = 1$ and $\gamma = 2$. It is seen that curves of the energies as functions of the electric field exhibit multiple crossovers and a reordering of the energy levels. As a consequence the slope of the curve for the ground state energy is changed abruptly for the electric field $F = -0.4$ kV/cm when $\gamma = 1$ and for $F = -0.2$ kV/cm when $\gamma = 2$, causing a jump of the electric dipole momentum at these points. Also, it is seen that multiple crossovers of the energy levels with different magnetic momenta produces an oscillation of the parameters of the magnetic polarization in the second and third rows.

4. Summary and Conclusions

In order to analyze the effect of the electric and magnetic fields applied along the symmetry axis of type-II nanocone on the spectral and magnetic properties of the on-axis donor, we consider a separable model, in which it is supposed that the excessive electron released by the donor is located within a very narrow layer over lateral side of the structure. We show that the energies and the probability distributions of the electron along the symmetry axis in states with different angular momenta are defined mainly by the interplay between the centrifugal and diamagnetic forces. The centrifugal force pushes the maxima of the electron distributions with different angular momenta toward the cone's bottom, while the diamagnetic force drives them to the cone top. As the magnetic field is small, the centrifugal force retains the electron rotation around the axis close to the bottom. When the magnetic field is increased, the peaks of the electron distributions corresponding to different angular momenta begin to climb successively one by one from base toward the top, pushed up by the diamagnetic force, in the order of the ascending angular momenta.

We show that such redistribution of the electron's probability density produces a consistent decrease of the amplitude and the period of the AB oscillations of the ground state energy as function of the magnetic field, which are different from those in a narrow ring due to the presence of a linear growing trend of the bands' bottoms. The amplitude, the period, and the slope of the envelope line over the ground state energy for the positive electric field is lesser than for negative one and it tends to zero in the presence of a very strong electric field. Thus, the electric field can obstruct or can stimulate a climb of the electron circular tracks, generated by the increasing magnetic confinement, varying the magnetic

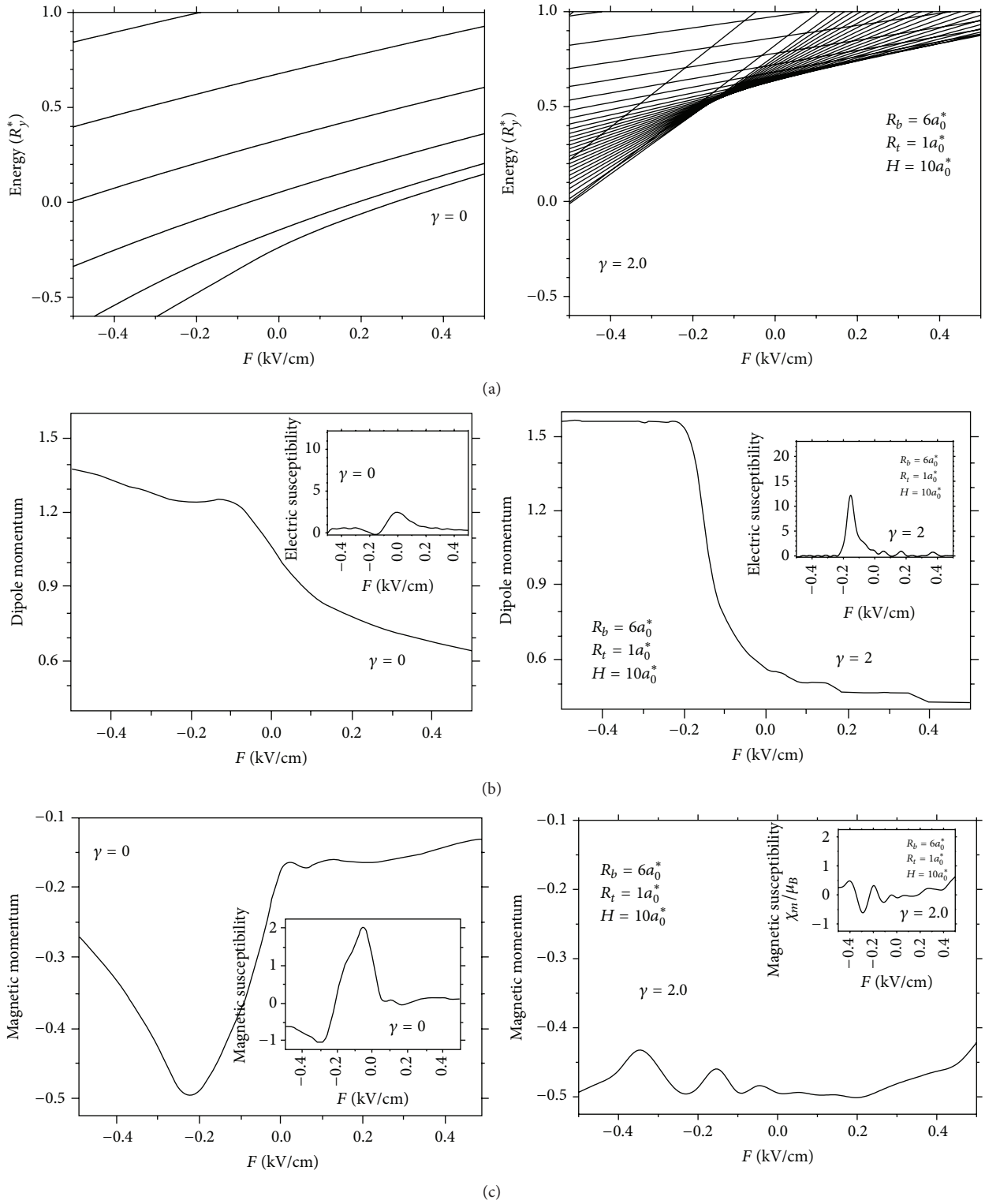

Figure 5: The lower energies and parameters of the electric and magnetic polarizations as functions of the external electric field in one-electron conical nanotube for three different values of the magnetic field.

momentum and the magnetic polarizability of the system. The climb of the circular tracks with different magnetic momenta can be also produced by increasing the electric field, changing abruptly the dipole moment.

Our theoretical analysis reveals a new possibility for the coupling between the polarization and magnetization arising from the quantum-size effect in type-II semiconductor nanocones.

Competing Interests

The authors declare that there is no conflict of interests regarding the publication of this paper.

Acknowledgments

This work was financed by the Universidad del Magdalena through Vicerrectoría de Investigación and the Universidad Industrial de Santander (UIS) through Vicerrectoría de Investigación y Extensión, DIEF de Ciencias (Cod. 1350).

References

[1] J. Zhai, J. Li, D. Viehland, and M. I. Bichurin, "Large magnetoelectric susceptibility: the fundamental property of piezoelectric and magnetostrictive laminated composites," *Journal of Applied Physics*, vol. 101, Article ID 014102, 2007.

[2] Y. Yang, J. Íñiguez, A.-J. Mao, and L. Bellaiche, "Prediction of a novel magnetoelectric switching mechanism in multiferroics," *Physical Review Letters*, vol. 112, no. 5, Article ID 057202, 2014.

[3] C.-M. Hsu, C. Battaglia, C. Pahud et al., "High-efficiency amorphous silicon solar cell on a periodic nanocone back reflector," *Advanced Energy Materials*, vol. 2, no. 6, pp. 628–633, 2012.

[4] S. Jeong, E. C. Garnett, S. Wang et al., "Hybrid silicon nanocone-polymer solar cells," *Nano Letters*, vol. 12, no. 6, pp. 2971–2976, 2012.

[5] K. Wang, J. Chen, W. Zhou et al., "Direct growth of highly mismatched type II ZnO/ZnSe core/shell nanowire arrays on transparent conducting oxide substrates for solar cell applications," *Advanced Materials*, vol. 20, no. 17, pp. 3248–3253, 2008.

[6] H.-M. Lin, Y.-L. Chen, J. Yang et al., "Synthesis and characterization of core-shell GaP@GaN and GaN@GaP nanowires," *Nano Letters*, vol. 3, no. 4, pp. 537–541, 2003.

[7] A. V. Chaplik, *JETP Letters*, vol. 62, p. 900, 1995.

[8] A. V. Chaplik, *Journal of Experimental and Theoretical Physics*, vol. 92, p. 169, 2001.

[9] V. M. Fomin, Ed., *Physics of Quantum Rings*, Springer, Berlin, Germany, 2014.

[10] L. Wendler, V. M. Fomin, A. V. Chaplik, and A. O. Govorov, "Optical properties of two interacting electrons in quantum rings: optical absorption and inelastic light scattering," *Physical Review B*, vol. 54, pp. 4794–4810, 1996.

[11] M. Bayer, "Exciton complexes in self-assembled In(Ga)As/GaAs quantum dots," in *Single Quantum Dots: Fundamentals, Applications, and New Concepts*, P. Michler, Ed., pp. 93–146, Springer, Heidelberg, Germany, 2003.

[12] F. J. Betancur, I. D. Mikhailov, and L. E. Oliveira, "Shallow donor states in GaAs-(Ga, Al)As quantum dots with different potential shapes," *Journal of Physics D: Applied Physics*, vol. 31, no. 23, pp. 3391–3396, 1998.